

A REVIEW OF HIGH RESOLUTION MODELING STUDIES OF THE EXCHANGE FLOWS OF THE TURKISH STRAITS SYSTEM

Adil SÖZER ^{1,2}, Gianmaria SANNINO ³ and Emin ÖZSOY ^{1,4}

¹ Institute of Marine Sciences, Middle East Technical University, Mersin, Turkey

² Fatsa Faculty of Marine Sciences, Ordu University, Ordu, Turkey

³ Energy and Environmental Modeling Unit (ENEA), Rome, Italy

⁴ Eurasia Institute of Earth Sciences, İstanbul Technical University, İstanbul, Turkey
ozsoyem@itu.edu.tr

1. Introduction

Constructing a model of the entire TSS uniformly representing the rich diversity of observed hydrodynamic processes including strong topographic control, non-linear hydrodynamics, strong stratified turbulence, hydraulic controls, separated flows, multi-scale interactions, turbulent mixing and entrainment has been a *grand challenge* in oceanography that we have approached in small steps. In the past, the problem has only been addressed by a series of simplified models of the individual elements of the system (e.g. Oğuz *et al.* 1990; Ilıcak *et al.* 2009; Oğuz and Sur; 1989; Staschuk and Hutter, 2001). In this paper, we review the earlier work (Sözer, 2013; Sannino *et al.* 2015) carried out with three-dimensional models of the individual Bosphorus Strait or the coupled dynamics of the TSS, momentarily skipping some details and updates already submitted for publication (Sözer and Özsoy, 2016; Sannino *et al.* 2016). We will only review some salient features and partial results that have not been discussed in those journal papers.

2. Model Development

2.1 ROMS Model for the Bosphorus Strait

The modeling of the Bosphorus Strait hydrodynamics is based on the ROMS, a well-documented and tested community model (Hedström, 1997; Haidvogel *et al.* 2000; Shchepetkin and McWilliams, 2005). Models with both idealized and realistic geometry versions have been used to study the Bosphorus Strait (Sözer 2013).

The idealized geometry of the Bosphorus Strait (Figure 1a) is a straight channel ~34 km in length, 70m in depth and 1300 m in width, with a contraction of 700 m width located at one-third of its length and a sill of 500 m length and 57 m depth at the crest located near the lower density end of the strait represented on a 55x512x35 rectilinear grid of $\Delta x = \Delta y = 100$ m with variable vertical spacing of $\Delta z = 1.42 - 2.0$ m in generalized s-coordinates. For simplicity, only salinity effects are included. Constant horizontal and vertical diffusivity values of $15 \text{ m}^2/\text{s}$ and $10^{-4} \text{ m}^2/\text{s}$ are respectively used for momentum and tracers. For the realistic geometry model (Figure 1b), high resolution bathymetric

data of Göktaşan (2005) have been first resampled and interpolated to a variable resolution rectilinear grid of 163x716 nodes with $\Delta x = 50 - 200$ m, $\Delta y = 50 - 325$ m and 35 s-levels with vertical spacing of 0.7 - 2.85 m. The Generic Length-Scale (GLS) turbulence scheme with the k-epsilon formulation and radiation boundary conditions were used for flow variables at the north and south open boundaries. High order advection schemes, volume-conservation at open boundaries, non-linear equation of stat, and Smagorinsky formulation of lateral diffusive effects on constant geopotential surfaces have been used. In both models, 2d velocity has been prescribed at the southern boundary to force the net flow. No-slip boundary conditions and quadratic bottom friction (RDRG2 = 0.005) and recursive advection scheme to minimize effects of sharp gradients have been used.

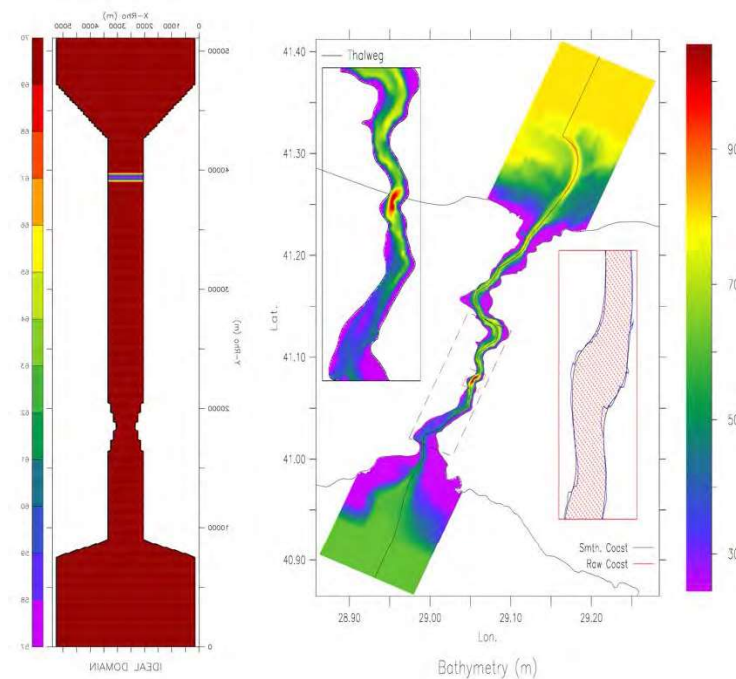


Figure 1. ROMS model configuration for (a) idealized and (b) realistic geometry models of the Bosphorus.

2.2 MITgcm Model for the Turkish Straits System

The Massachusetts Institute of Technology general circulation model (MITgcm) is used to study the entire TSS, including adjacent areas of the northeast Aegean Sea and the Black Sea. A non-uniform curvilinear orthogonal grid (1728×648), tilted and stretched at the Bosphorus and Dardanelles Straits covers the domain at variable resolution of 50 m at Straits to about 1 km in the Marmara Sea, with 100 vertical z-level steps in the range of 1.2 m - 80 m. (Figure 2).

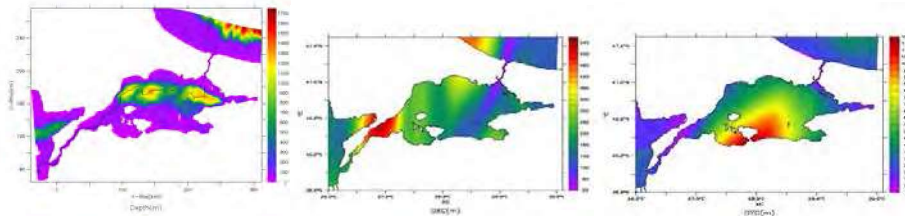


Figure 2. (a) Model topography (depth in m, solid line is the thalweg), and step size of model horizontal discretization (m) in (b) lengthwise and (c) transverse directions.

The model is initialized with lock exchange initial conditions represented by three vertical profiles of properties obtained during June-July 2013. No-slip conditions, high order tracer advection and turbulent closure parametrization scheme of Pacanowski and Philander [1981], with horizontal diffusivity of $10^{-2} \text{ m}^2\text{s}^{-1}$, and variable horizontal viscosity following Leith [1968] have been used.

3. Model Results

3.1 Bosphorus Model - Exchange Flows

With the model started from non-uniform, stratified boundary conditions at the two ends of the strait approximating September 1994 observations of Gregg and Özsoy (2002), a steady solution is reached after several cycles of adjustment oscillations, as shown in Figure 3. The Cold Intermediate Water (CIW) of the Black Sea entering below the warm mixed layer (Figure 3a) comes in contact with the warmer waters of the undercurrent at the interface, modifying the turbulence properties of the flow, while the salinity stratification also contributes to these properties (Figure 3b). The vertical viscosity computed from the turbulence closure scheme (Figure 3c) indicates turbulent patches in the upper and lower layers of the flow with greatly reduced values at the interfacial layer, where the turbulence is suppressed by the density stratification.

The model solutions qualitatively reproduce many features reported in the earlier observations (e.g. Özsoy *et al.* 2001; Gregg and Özsoy, 2002), such as the wedge shape of the upper and lower layers of rather uniform properties, the thickness and depth of the mixing interfacial layer between them, the apparent hydraulic controls at the contraction and sill, the thin surface layer outflow into the Marmara Sea, the sill overflow and subsequent adjustment on the Black Sea shelf. Boundary conditions are able to establish and preserve the intended stratification in the neighboring Seas.

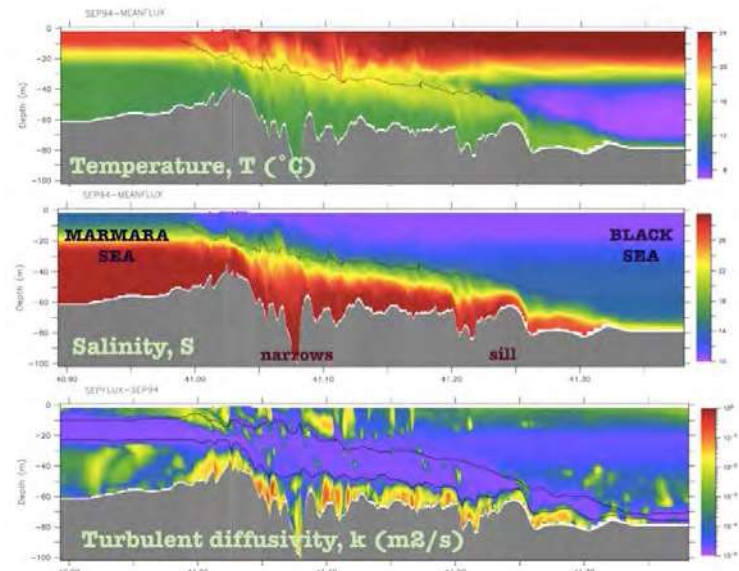


Figure 3. An example of a lock-exchange solution with stratified initial conditions at the two end reservoirs of the Bosphorus: (a) temperature, (b) salinity and (c) turbulent diffusivity along the Strait, following the thalweg.

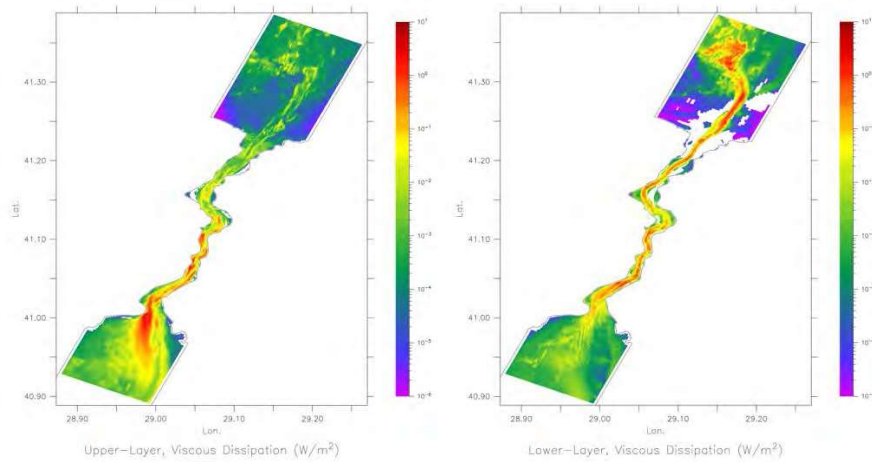


Figure 4. Horizontal distribution of the mechanical energy dissipation by turbulence in the (a) upper layer and (b) lower layer.

The horizontal distribution of the upper and lower layer mechanical energy dissipation rates shown in Figure 4 confirm dissipation at the various bends and along the bottom by friction, at the surface jet issuing into the Marmara Sea, past the northern sill and along the bottom plume on the Black Sea shelf. Total dissipation values of $\sim 10.1\text{Mw}$ and $\sim 7.3\text{Mw}$ were found for the upper and the lower layers respectively, for the entire model domain.

3.2 Hydraulic Control

Because the hydraulic control issue deserves extensive discussion expounded upon in the relevant papers (Sözer and Özsoy, 2016; Sannino *et al.* 2016) we only provide a very brief description of the horizontal distributions of the two-layer composite densimetric Froude number $\mathbf{G}^2 = \mathbf{F}_{1w}^2 + \mathbf{F}_{2w}^2$ where $\mathbf{F}_{iw}^2 = \mathbf{u}_i^2/\mathbf{g}'\mathbf{h}_i$ are the local layer Froude numbers for lower layers $i=1,2$ respectively, where \mathbf{u}_i is the layer average current speed and \mathbf{h}_i the depth, $\mathbf{g}' = \mathbf{g} \Delta\rho/\rho$ is the reduced gravity with density ratio $\Delta\rho/\rho$.

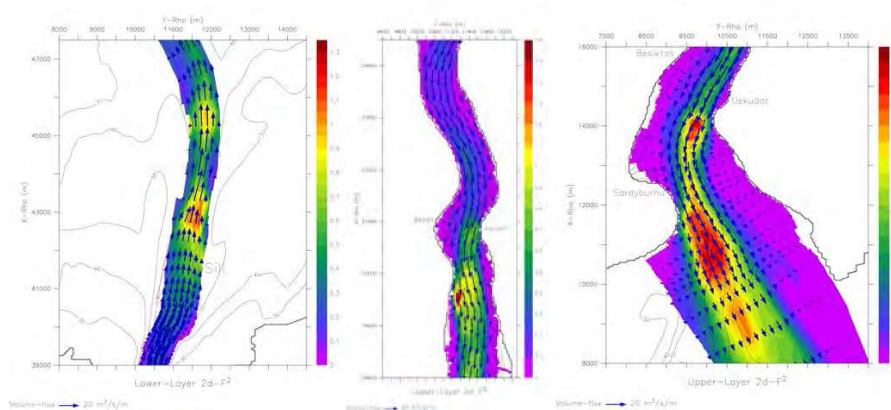


Figure 5. Froude number in the (a) lower-layer past the northern sill, (b) upper layer in the contraction region and (c) upper layer at the Marmara Sea exit of Bosphorus.

We leave the details of the Froude number discussion to the respective papers quoted above. We only note that the demonstration of hydraulic controls at the relevant sections of the straits is a very delicate matter that requires successive levels of approximations.

3.3 Response to barotropic forcing

Either a velocity based two-layer decomposition assigning upper / lower layer volume fluxes to oppositely directed components \mathbf{Q}_1 and \mathbf{Q}_2 is used, or a three-layer decomposition assigning the top, interfacial and bottom layers \mathbf{Q}_T , \mathbf{Q}_I and \mathbf{Q}_B respectively using salinity to separate layers is preferred, where layer limits are defined by 10% difference from the top and bottom values.

In Figures 5 and 6 we display the changes that occur continuously in the Bosphorus exchange flow as the net flux is changed. These simulations are performed by successive initializations of the model starting from the stratified central run with a barotropic flux of $\mathbf{Q} = 9.5 \times 10^3 \text{ m}^3/\text{s}$, and in each case running at least for about 7 days to reach steady state solutions. The top, interfacial and bottom layer volume fluxes \mathbf{Q}_T , \mathbf{Q}_I , and \mathbf{Q}_B

respectively calculated at the mid-strait section and identified by local salinity limits are shown with the heavy arrows in Figure 5 and 6.

Increasing the flow to take on positive values of the net flux (towards the Marmara Sea) in Figure 5, the upper layer flow becomes increasingly dominant to both the interfacial and lower layers, finally leading to the case where the lower layer becomes blocked, as observed in the measurements, e.g. Latif *et al.* (1991). The zero-velocity line for low negative fluxes coincide with the center of the interfacial layer and rises above it in the north, while with increasing positive flux, the isotach becomes deeper and aligned with the lower demarcation of the interface layer. It is noteworthy, however, that the switch to the blocking situation occurs very suddenly as the barotropic forcing is increased, for instance from the unblocked case just before the last one in Figure 6. The zero velocity isotach is depressed below the salinity interfacial layer for the stronger levels of barotropic forcing.

We start in Figure 6 with the case in which the upper layer completely blocked by an extreme negative net flux (towards the Black Sea). In this case, because the upper layer is blocked in the form of a wedge and pushed all the way up north past the contraction region, the flow is configured with three-layer stratification in the Strait, where the upper layer Marmara waters flowing north and forming the thick interface layer are pushed under the wedge of former upper layer waters originally invading the Strait from the Black Sea. The zero-velocity isotach for this extreme flux is much separated from the salinity interface and has lifted closer to the surface in the northern part of the strait. The three-layer structure in which the interfacial and bottom layers are co-flowing against the retreating top layer flow in this extreme case is similar to what has been noted in earlier measurements, e.g. Latif *et al.* (1991). As the positive flux is gradually decreased first the blocked wedge of the original Black Sea upper layer retreats until the southern exit when the interfacial layer of Marmara Sea water becomes thinner and carries less transport, till after that the upper layer flow starts to build up at the cost of the interfacial layer which gets thinner and starts to get an equal share of flux with the lower layer when the net flux approaches zero. In most positive flux experiments excluding the upper layer blocked cases the zero velocity isotach is above the interfacial layer, meaning that the interfacial and lower layers act in unison.

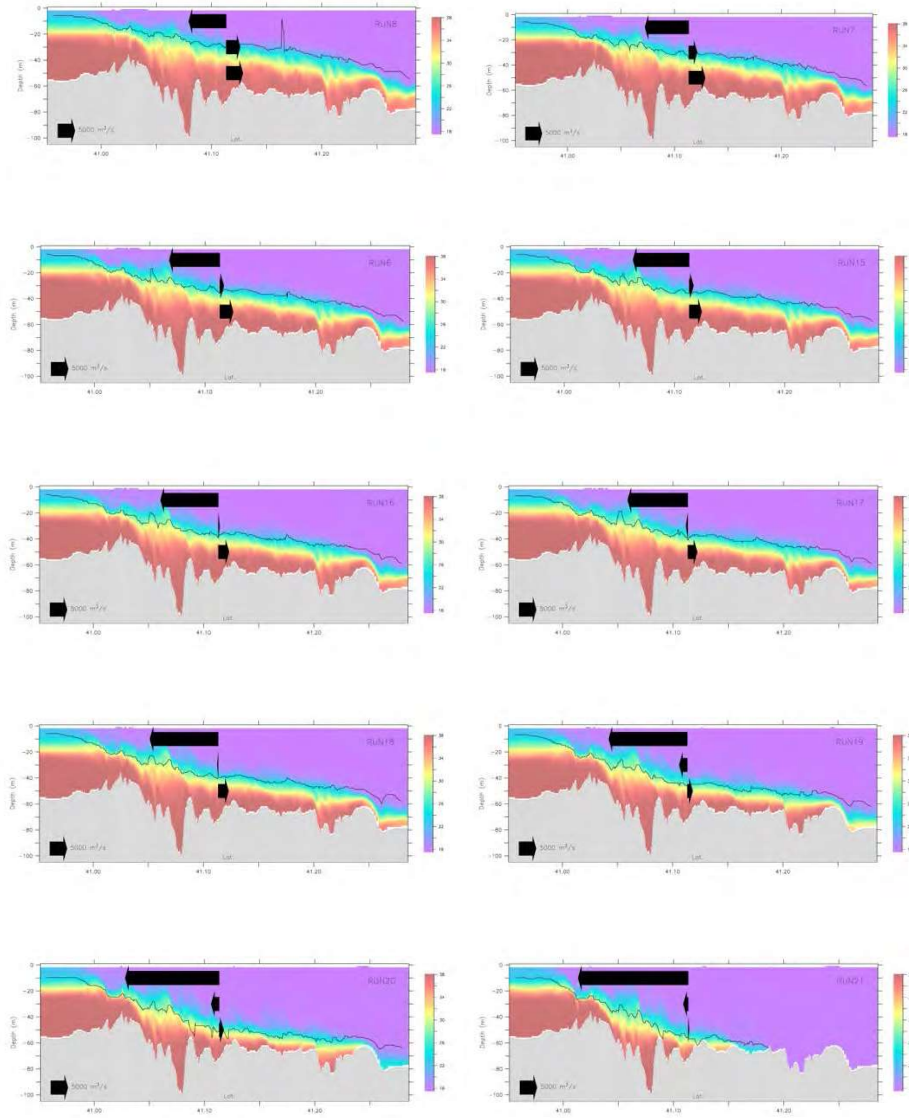


Figure 6. The salinity distribution, the zero velocity isotach, and arrows showing the relative magnitudes of the top, interfacial and bottom layer fluxes for increasing positive net flux values of $Q= 1900, 5700, 9500, 11400, 13300, 15200, 17000, 23700, 28400, 33200 \text{ m}^3/\text{s}$ (towards the Marmara Sea). The layer fluxes are compared to a scale arrow of $5000 \text{ m}^3/\text{s}$ at the bottom of each plot.

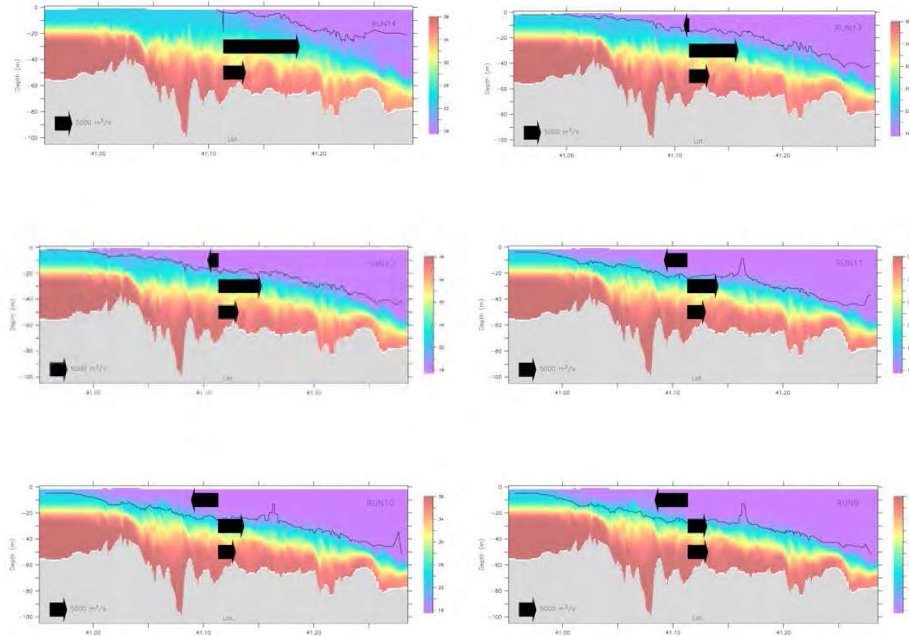


Figure 7. The salinity distribution, the zero velocity isotach, and arrows showing the relative magnitudes of the top, interfacial and bottom layer fluxes for decreasing negative net flux values of $Q = -28500, -19000, -15200, -7600, -4700, -1900 \text{ m}^3/\text{s}$ (towards the Black Sea). The layer fluxes are compared to a scale arrow of $5000 \text{ m}^3/\text{s}$ at the bottom of each plot.

3.4 Bosphorus sea level difference and exchange fluxes

Historical and modern measurements seem to agree on sea-level differences of 30-60 cm across the entire TSS, and 20-60 cm across the Bosphorus (Marsili 1681; Möller 1928; Smith 1942; Gunnerson and Özturgut 1986; De Filippi *et al.* 1986; Büyükay 1989; Alpar and Yüce 1998; Özsoy *et al.* 1998; Gregg and Özsoy, 1999; Yüksel *et al.* 2008). Gregg *et al.* (1999) found rapid, nonlinear changes of sea level near the contraction of the Bosphorus in parallel to the changes in the depth of the density interface. Similar behavior is discovered in our model simulations (Figure 7), with the largest changes in free-surface height occurring at the Marmara Sea junction and at the contraction region, in consequence of the hydraulic control at these locations. The final elevation difference between the two ends of the strait is about 26-40 cm in various runs with stratified boundary conditions amounting to the smaller density difference between the two seas, comparable with the values measured by Gregg and Özsoy (2002) during the moderate flow conditions of September 1994.

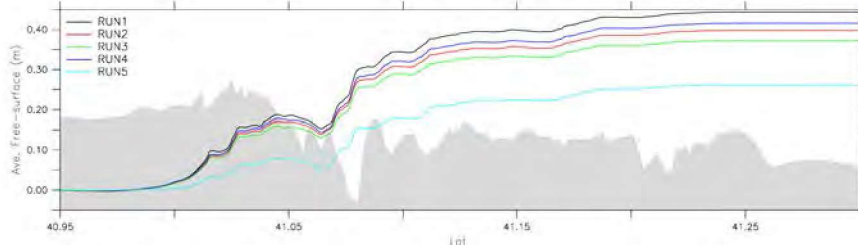


Figure 8. Sea level changes along the Bosphorus for various runs in Sözer (2013) (bathymetry in the background).

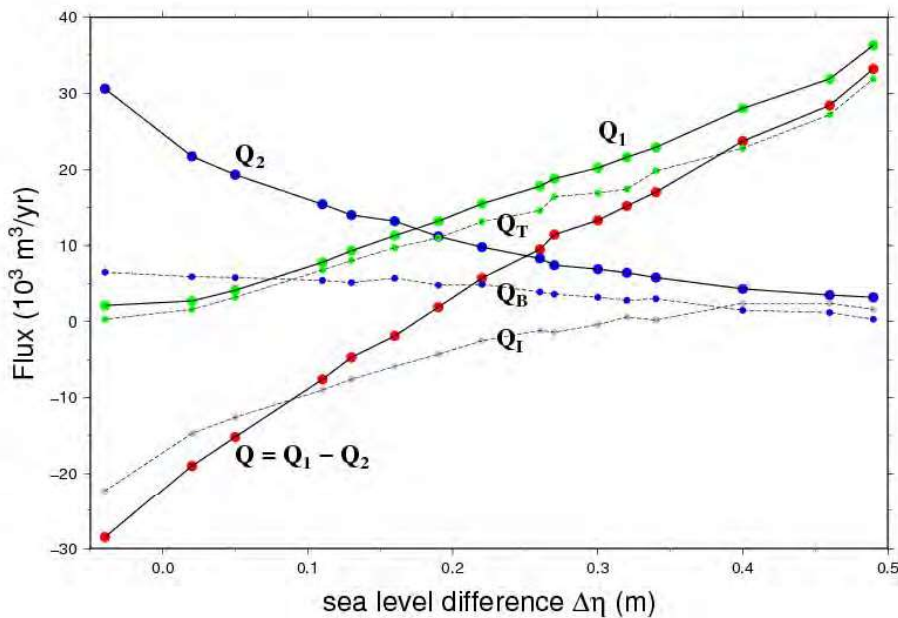


Figure 9. The variation of the net barotropic flux Q (red, solid line), and two-layer fluxes in the upper layer, Q_1 (green, solid), lower layer, Q_2 (blue, solid), three-layer fluxes in the top layer, Q_T (green, dashed), bottom layer, Q_B (blue, dashed) and interfacial layer, Q_I (gray, dashed), with sea level difference $\Delta\eta$. (Q_T , Q_T and Q_I are positive southward, Q_2 and Q_B are positive northward, and $\Delta\eta$ is the sea level difference north-south).

The relationships between the sea level differential $\Delta\eta$ across the Bosphorus and the net barotropic flux Q , together with the two and three layer fluxes are provided in Figure 8, based on the model runs summarized in Figure 6. Blocking of the lower layer occurs for a net flux of $Q = 33200 \text{ m}^3/\text{s}$ out of the Black Sea resulting in a sea level difference of $\Delta\eta = 0.49\text{m}$, and for the upper layer blocked case of $Q = -28500 \text{ m}^3/\text{s}$ the sea level difference is negative, $\Delta\eta = -0.04 \text{ m}$, i.e. close to zero. The relationship between

net flow Q and the sea level difference $\Delta\eta$ is close to a linear one except close to blocking. The variations of the two-layer fluxes Q_1 , and Q_2 , and the three layer fluxes Q_T , Q_I , and Q_B are sketched in Figure 7, with $Q = Q_2 - Q_1 = Q_T + Q_I - Q_B$ by definition. The bottom layer flux is not much sensitive to changes in sea level.

Upper layer fluxes estimated from current measurements from a bottom mounted cabled ADCP at Baltalimanı in the Bosphorus and sea level monitored at coastal stations at Şile on the Black Sea and Yalova on the Marmara Sea coasts during the years 2008-2012 (Tutsak, 2013) low-pass filtered at 30h are compared in Figure 9. Despite deviations between measurements and model results, a rough comparison is made between the independent estimates. It is also interesting to note that monthly average sea level differences of Tutsak (2013) varied in the range of 15-30 cm for Şile-Yalova stations with respect to the Bosphorus, and 30-40 cm for Yalova-Gökçeada stations with respect to the Dardanelles Straits.

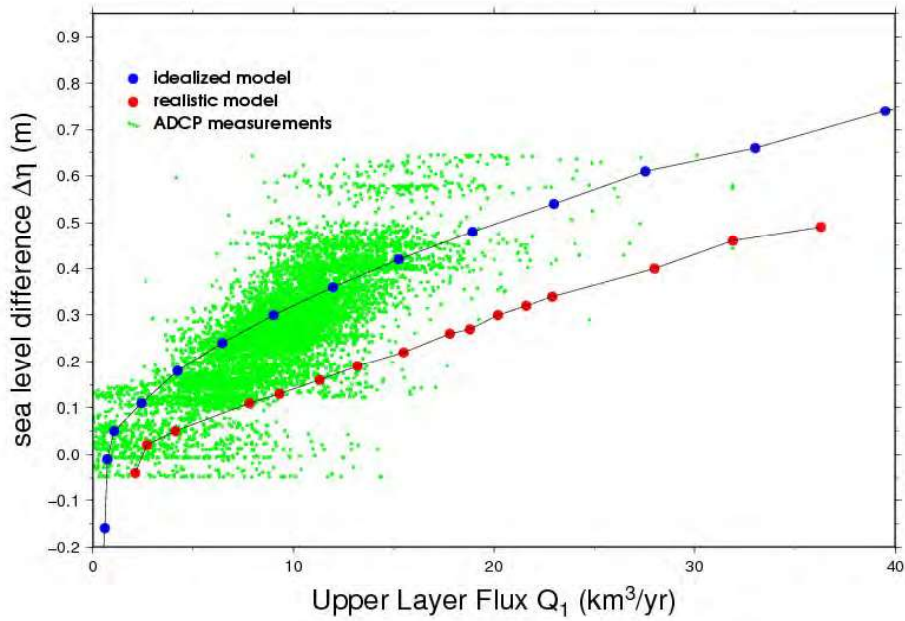


Figure 10. The relationship between upper layer flux Q_1 and sea level difference $\Delta\eta$ based on idealized (blue) and realistic (red) geometry Bosphorus model results and measurements of ADCP current profiles integrated across the flow area at Baltalimanı versus the sea level difference Şile – Yalova (green) during 2008-2012.

3.5 MITgcm Model of the Turkish Straits System

The non-uniform curvilinear orthogonal grid and the vertical resolution implemented in the MITgcm model have demonstrated to be sufficient to capture the fine scales within the two Straits and also to well represent mesoscale in the Marmara Sea. We only review basic results here and leave the rest to Sannino *et al.* (2016). The response of the currents and density structure over the water column to different net flow is also examined through the setup of experiments with varying net barotropic volume flux values of $Q = -9600, 0, 5600, 9600, 18000$ and $50000 \text{ m}^3/\text{s}$ respectively (positive values represent flow from the Black Sea towards the Mediterranean).

For the studied flows driven solely by the net flux, an S-shaped current first moving south from the Bosphorus, later turning northwest and finally exiting from the Dardanelles Strait appears to be the basic character of the circulation. With a negative flux of $Q = -9600 \text{ m}^3/\text{s}$ towards the Black Sea, the upper layer flow is still positive, and sufficient to generate an anticyclonic net circulation in the midst of the Marmara Sea, as shown in Figure 10. For zero net flux, the same structure is preserved and as the positive values of the barotropic flux is increased further the size of the central gyre is reduced and the flow becomes increasingly more attached to the northern coast of the Marmara Sea. As the flux is increased to $9600 \text{ m}^3/\text{s}$, the central anticyclonic circulation cell takes an elongated form. For the extreme flux values of $Q = 18000 \text{ m}^3/\text{s}$ and $Q = 50000 \text{ m}^3/\text{s}$, the lower layer flow in the Bosphorus becomes blocked, and qualitative changes occur in the circulation of the Marmara Sea, with a smaller anticyclone near the Bosphorus exit, a jet attached to the northern coast, and a secondary anticyclone further west, and a cyclonic circulation emerging in the south. For these cases, the circulation pattern looks more like the buoyancy driven flow along the coast adjacent to the mouth of a river.

The generation of a basic anticyclonic circulation in the Marmara Sea for lower net fluxes, evolving towards a more balanced circulation of cyclonic-anticyclonic eddies appears to be a result of the vorticity balance of the basin. As shown by Spall and Price (1998), and studied by Morrison (2011), the net basin circulation is sensitively determined by the potential vorticity (PV) imports and exports of the basin. From this point of view, the reduction of interface depth (or upper layer thickness) from the Black Sea to the Marmara Sea implies a decrease in fluid vorticity, or anticyclonic circulation assuming the input to have zero vorticity.

The behaviour of the buoyant plume entering the Marmara Sea, initially shooting south and hitting the opposite coast is displayed in all cases in Figure 10, although the later turning of the flow to the west is typical of buoyant plumes at this scale. Buoyant flows entering the sea are typically attached to the right hand coast (looking out from the exit in the northern hemisphere, especially for initial vorticity zero below a critical limit

(e.g. Nof, 1978, Stern *et al.* 1982). Often a bulge of the buoyant fluid is formed, as the flow turns right to follow the coast, as often observed at river mouths (e.g. Huq, 2013).

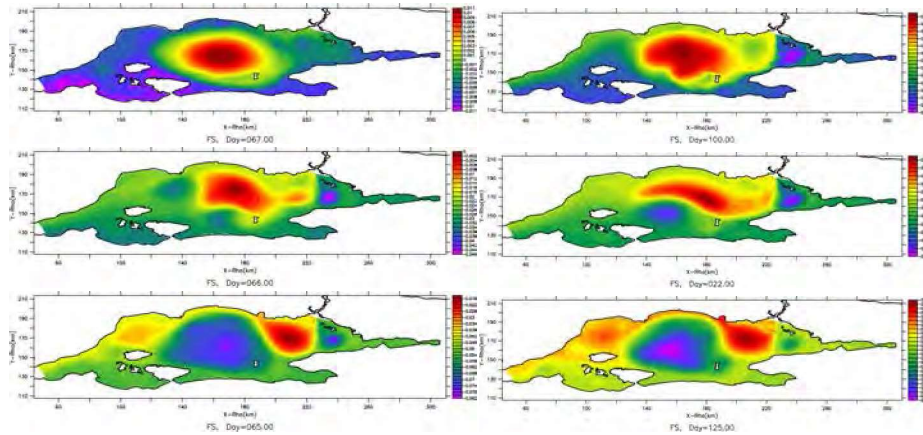


Figure 11. The free surface variations in the Marmara Sea for varying net barotropic volume flux values and total days of run for $Q = -9600$ (day=67), $0 \text{ m}^3/\text{s}$ (day 66), $5600 \text{ m}^3/\text{s}$ (day 100), $9600 \text{ m}^3/\text{s}$ (day 22), $18000 \text{ m}^3/\text{s}$ (day 65) and $50000 \text{ m}^3/\text{s}$ (day125).

In a two-layer system with variable bottom topography and dynamically active layers, the circulation may develop differently, with topography influencing the lower layer flow, and the resultant interface topography influencing the upper layer flow (Beardsley and Hart, 1978). As the net flux is increased in Figure 10, the changes in the circulation pattern may be a result of this kind of interactive adjustment of the flow layers to bottom and interface topography.

The qualitative change in the circulation towards a series of anticyclonic and cyclonic eddies following the meander of the currents, when the flux is increased to $18000 \text{ m}^3/\text{s}$ and $50000 \text{ m}^3/\text{s}$ is reminiscent of the Alboran Sea, where similar gyres filling the basin develop under high fluxes (Spall and Price, 1998; Riha and Peliz, 2013).

The sea level differences that develop at the two straits, Bosphorus and Dardanelles are given in Table 1, in relation to the net barotropic fluxes and the values obtained from the TSS model are compared with the ROMS model results for the Bosphorus (Sözer, 2013). While the total range of sea level in the Marmara Sea between cyclonic and anticyclonic areas varies between 2-12 cm (Figure 10), the net sea level differences across straits are much larger, varying between 2-85 cm in the Bosphorus and 1-32 cm in the Dardanelles, while the results for the Bosphorus compare well between the two models. These results would imply sea level differences of about 0-120 cm between the Black Sea and the Aegean Sea, for the range of net transport tested.

Table 1. Sea Level Difference at Straits as a Function of Net Flux

Net flux Q (m ³ /s)	Bosphorus (TSS) Sea level difference $\Delta\eta$ (cm)	Dardanelles (TSS) sea level difference $\Delta\eta$ (cm)	Bosphorus (ROMS) sea level difference $\Delta\eta$ (cm)
-9600	2	1.5	-
0	8	5	14
5600	10	7	18
9600	14	11	22
18000	22	16	30
50000	85	32	-

The salinity cross-sections throughout the TSS are shown in Figure 11, following the thalweg line of Figure 2a, for selected net barotropic flux values. The upper layer thickness remains around 25 m for fluxes up to 9600 m³/s, and increases to 35 m at the maximum flux value of 50000 m³/s. The upper layer reflects modified Black Sea characteristics while the lower layer reflects Mediterranean characteristics all along the transect, while the most rapid changes in salinity occur in the Bosphorus and Dardanelles straits, by mixing between the two water masses, as also indicated by observational results (Beşiktepe *et al.* 1993). The interface depth also varies strongly in the two straits, where fast exchange currents subject to hydraulic controls at transition areas (Gregg *et al.* 1999; Gregg and Özsoy 1999, 2002; Özsoy *et al.* 2001; Ilıcak *et al.* 2009; Sözer 2013).

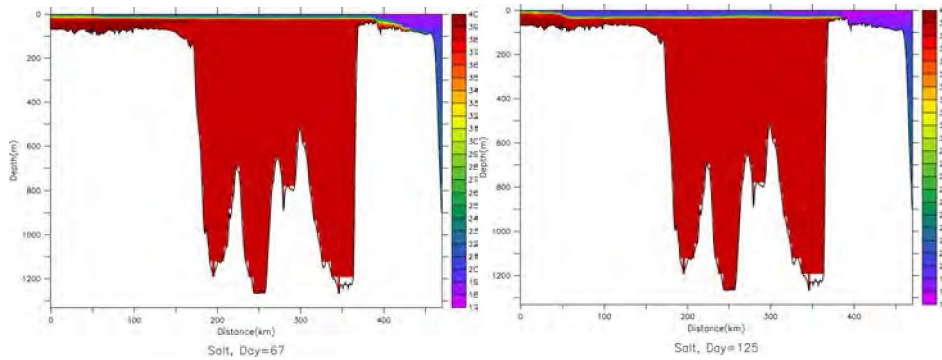


Figure 12. Salinity cross-sections along the thalweg line of Figure 2a in the Marmara Sea for selected net barotropic volume flux values of $Q = -9600$ and 50000 m³/s.

Below the sharp pycnocline of the Marmara Sea, properties are rather uniform, except very near the interface where an injection of more saline water from the Dardanelles spreads below the halocline. The spread below the halocline is typical for the summer season of June 2013 for which the model has been initialized. However, the appearance of denser waters at winter time would change this pattern as the dense water

sinks to the westernmost depression of the Marmara Sea and spreads along the bottom (Beşiktepe *et al.* 1993, 1994; Hüsrevoğlu 1999).

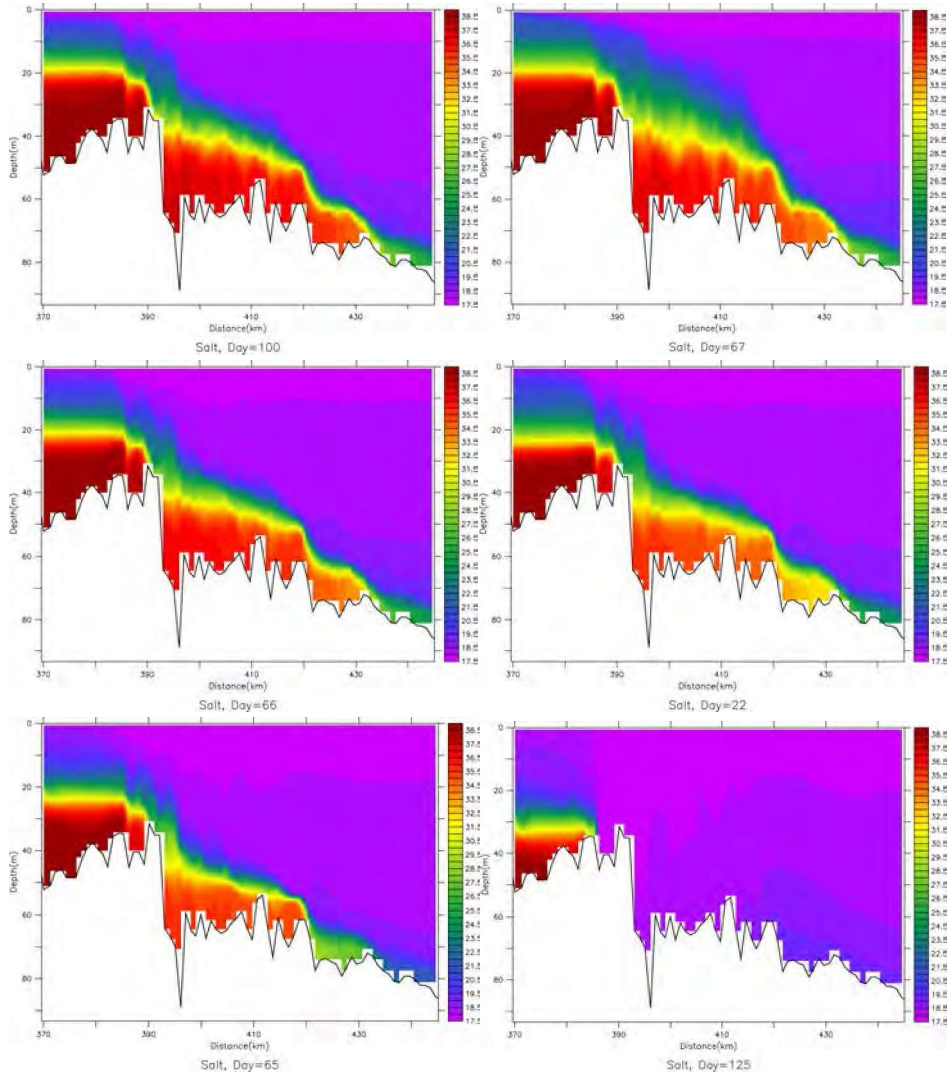


Figure 13. Salinity cross-sections across the Bosphorus along the thalweg in Figure 2a, for varying net barotropic volume flux values of $Q = -9600, 0, 5600, 9600, 18000$ and $50000 \text{ m}^3/\text{s}$.

The expanded views of salinity cross-sections for the Bosphorus and Dardanelles are respectively shown in Figures 12 and 13. The cross sections in Figures 12 and 13 confirm the existence of hydraulic transitions at expected hydraulic control sections based on past observations, also better resolved by higher resolution local models of the straits

(Gregg *et al.* 1999; Gregg and Özsoy, 1999, 2002; Özsoy *et al.* 2001; Ilıcak *et al.* 2009; Sözer 2013).

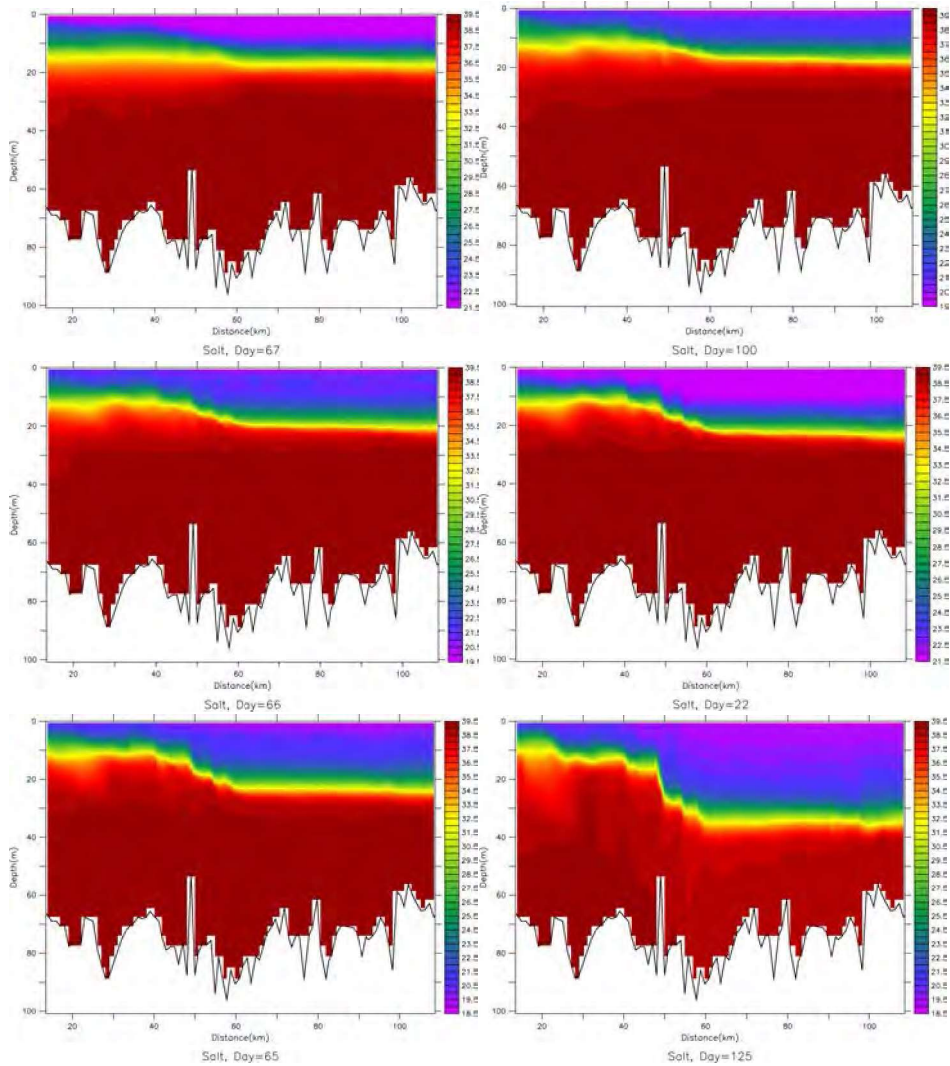


Figure 14. Salinity cross-sections across the Dardanelles along the thalweg in Figure 2a, for varying net barotropic volume flux values of $Q = -9600, 0, 5600, 9600, 18000$ and $50000 \text{ m}^3/\text{s}$.

Because the TSS has distinct regions of varied geometrical properties with a wide range of dynamical processes active in these regions, the physical response is different in each region. The evolution of kinetic energy is shown in Figure 14 for different regions. It is observed that the approach to a steady state is very fast in the two straits, while the wider areas of the three adjacent basins respond much slower.

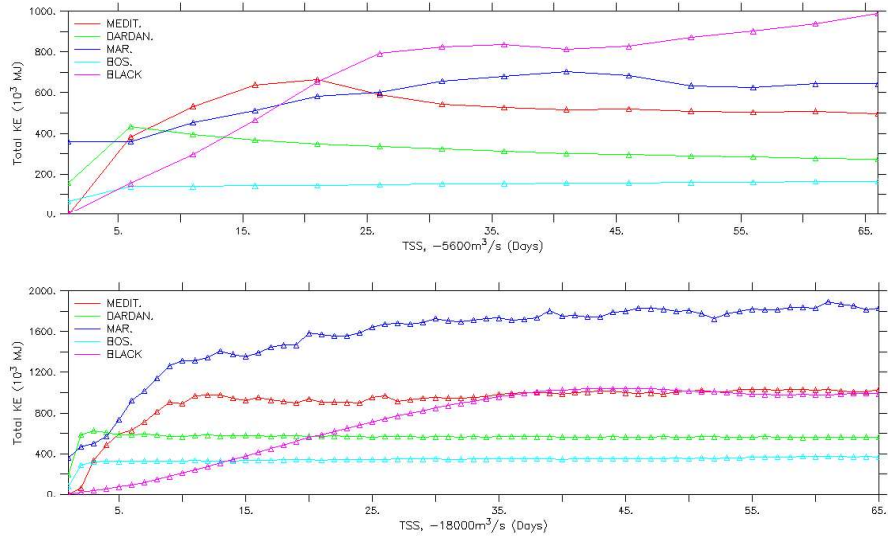


Figure 15. Evolution of kinetic energy for different regions of the TSS for selected values of net transport, $Q=5600$ and $18000 \text{ m}^3/\text{s}$.

Finally in Figure 15, a comparison is made of the upper-layer (Q_1) and lower-layer (Q_2) volume fluxes through the Bosphorus, based on observational data and the results from the Bosphorus model (ROMS) of Sözer (2013) and the TSS (MITgcm) models. Although the Bosphorus model is more specific to the Strait and has better resolution, the TSS model results perform even better in comparison with observations.

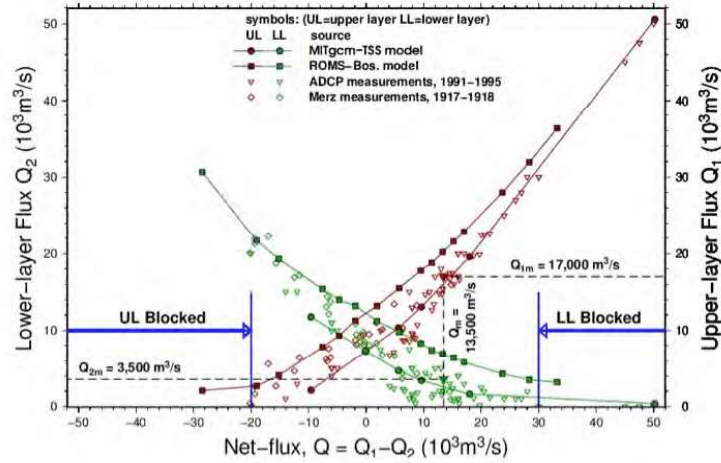


Figure 16. Upper-layer (Q_1) and lower-layer (Q_2) volume fluxes through the Bosphorus as a function of the and net flux ($Q=Q_1-Q_2$), based on observational data and compared with the results from the Bosphorus model (ROMS) of Sözer (2013) and the TSS (MITgcm) models.

References

- Alpar, B. and H. Yüce 1998. Sea-level variations and their interactions between the Black Sea and the Aegean Sea. *Estuarine Coastal and Shelf Science* 46: 609-619.
- Beardsley, R.C. and J. Hart 1978. A simple theoretical model for the flow of an estuary on to a continental shelf. *J. Geophys. Res.* 83:873-883.
- Beşiktepe, Ş., Özsoy, E. and Ü. Ünlüata 1993. Filling of the Marmara Sea by the Dardanelles lower layer inflow. *Deep-Sea Res.* 40: 1815-1838.
- Beşiktepe, Ş., Sur, H.İ., Özsoy, E., Latif, M.A., Oğuz, T. and Ü. Ünlüata 1994. The circulation and hydrography of the Marmara Sea. *Prog. Oceanogr.* 34: 285-334.
- Büyükay, M. 1989. The surface and internal oscillations in the Bosphorus, related to meteorological forces, M.Sc. Thesis, Institute of Marine Sciences, Middle East Technical University.
- De Filippi, G.L., Iovenitti, L. and A. Akyarlı 1986. Current analysis in the Marmara-Bosphorus Junction. 1st AIOM (Associazione di Ingegneria Offshore e Marina) Congress, Venice, June 1986, 5-25 pp.
- Gökaşan, E., Tur, H., Ecevitoglu, B., Görüm, T., Türker, A., Tok, B., Çağlak, F., Birkan, H. and M. Şimşek 2005. Evidence and implications of massive erosion along the Strait of İstanbul (Bosphorus). *Geo-Mar. Lett.* 25: 324-342.
- Gregg, M.C., Özsoy E. and M.A. Latif 1999. Quasi-steady exchange flow in the Bosphorus. *Geophys. Res. Lett.* 26: 83-86.

- Gregg, M.C. and E. Özsoy 1999. Mixing on the Black Sea shelf north of the Bosphorus. *Geophys. Res. Lett.* 26: 1869-1872.
- Gregg, M.C. and E. Özsoy 2002. Flow, water mass changes and hydraulics in the Bosphorus. *J. Geophys. Res.* 107 (C3):10.1029/2000JC000485.
- Gunnerson, C.G. and E. Özturgut 1974. The Bosphorus. In: American Association of Petroleum Geologists E.T. Degens, D.A. Ross (Eds) *The Black Sea – Geology, Chemistry and Biology* Tulsa, 103 pp.
- Haidvogel, D.B., Arango, H.G., Hedstrom, K., Beckmann, A., Malanotte-Rizzoli, P. and A.F. Shchepetkin 2000. Model evaluation experiments in the North Atlantic Basin: Simulations in nonlinear terrain-following coordinates. *Dyn. Atmos. Oceans* 32: 239-281.
- Hedström, K.S. 1997. Draft User's Manual for an S-Coordinate Primitive Equation Ocean Circulation Model (SCRUM) Version 3.0. Institute of Marine and Coastal Sciences, Rutgers University.
- Huq, P. 2013. Buoyant Outflows to the Coastal Ocean, *Handbook of Environmental Fluid Dynamics, Volume One*, H.J.S. Fernando (Ed). CRC Press / Taylor and Francis Group, LLC, 1:207-215.
- Hüsrevoğlu, Y.S. 1999. Modelling of the Dardanelles Strait lower-layer flow into the Marmara Sea, M.Sc. Thesis, Institute of Marine Sciences, METU, Erdemli, Mersin.
- Ilıcak, M., Özgökmen, T.M., Özsoy, E. and P.F. Fischer 2009. Non-hydrostatic modeling of exchange flows across geometries. *Ocean Complex Modeling* 29: 159–175.
- Jarosz, E., Teague, W.J., Book, J.W. and Ş. Beşiktepe 2011a. On flow variability in the Bosphorus Strait. *J. Geophys. Res.* 116: C08038. doi:10.1029/2010JC006861.
- Jarosz, E., Teague, W.J., Book, J.W. and Ş. Beşiktepe 2011b. Observed volume fluxes in the Bosphorus Strait. *Geophys. Res. Lett.* 38: L21608. doi:10.1029/2011GL049557.
- Jarosz, E., Teague, W.J., Book, J.W. and Ş.T. Beşiktepe 2012. Observations on the characteristics of the exchange flow in the Dardanelles Strait. *J. Geophys. Res.* 117: C11012. doi:10.1029/2012JC008348.
- Latif, M.A., Özsoy, E., Oğuz, T. and Ü. Ünlüata 1991. Observations of the Mediterranean inflow into the Black Sea. *Deep-Sea Res.* 38 (2): 711–723.
- Leith, C. 1968. Parameterization of vertical mixing in numerical models of tropical oceans. *Physics of Fluids* 10: 1409–1416.
- Morrison, A. 2011. Upstream Basin Circulation of Rotating, Hydraulically Controlled Flows, 2011 Summer Program in Geophysical Fluid Dynamics, WHOI, 429 pp.
- Möller, L. 1928. Alfred Merz' hydrographische Untersuchungen im Bosphorus und Dardanellen. Veröffentlichungen des Instituts für Meereskunde an der Universität Berlin. 18 (A): 284.
- Nof, D. 1978. On geostrophic adjustment in sea straits and wide estuaries: theory and laboratory experiments. Part II – two-layer system. *J. Phys. Ocean.* 8: 861-872.

- Oğuz, T. and H.İ. Sur 1989. A two-layer model of water exchange through the Dardanelles Strait. *Oceanology Acta* 12: 23-31.
- Oğuz, T., Özsoy, E., Latif, M.A., Sur, H.İ. and Ü. Ünlüata 1990. Modelling of hydraulically controlled exchange flow in the Bosphorus Strait. *Journal of Physical Oceanography* 20: 945-965.
- Özsoy, E., Latif, M.A., Beşiktepe, S., Çetin, N., Gregg, N., Belokopytov, V., Goryachkin, Y. and V. Diaconu 1998. The Bosphorus Strait: exchange fluxes, currents and sea-level changes. In: L. Ivanov, T. Oğuz (Eds) *Ecosystem Modeling as a Management Tool for the Black Sea*, NATO Science Series 2: Environmental Security 47 Kluwer Academic Publishers, Dordrecht, (1): 367 pp. + (2): 385 pp.
- Özsoy, E., Di Iorio, D., Gregg, M. and J. Backhaus 2001. Mixing in the Bosphorus Strait and the Black Sea continental shelf: observations and a model of the dense water outflow. *J. Mar. Sys.* 31: 99-135.
- Pacanowski, R. and S. Philander 1981. Parameterization of vertical mixing in numerical-models of tropical oceans. *J. Phys. Oceanogr.* 11(11): 1443-1451.
- Preller, R.H. 1986. A Numerical Model Study of the Alboran Sea Gyre. *Prog. Oceanogr.* 16(3):113-146.
- Riha, and Peliz 2013. A 2-layer primitive equation model of an idealized Strait of Gibraltar connected to an eastern basin. *Ocean Dynamics* 6: 615-631.
- Sannino, G., Sözer, A. and E. Özsoy 2016. A fine resolution modeling study of the Turkish Straits System. submitted for publication in *Ocean Dynamics*.
- Shchepetkin, A.F. and J.C. McWilliams 2005. The regional oceanic modeling system (ROMS): A split-explicit, free-surface, topography- following-coordinate oceanic model. *Ocean Modeling* 9: 347- 404.
- Sözer, A. 2013. Numerical Modeling of the Bosphorus exchange flow dynamics. Institute of Marine Sciences, Middle East Technical University, Erdemli, Mersin, Turkey, (unpublished Ph.D. thesis).
- Sözer, A. and E. Özsoy 2016. Modeling of the Bosphorus exchange flow Dynamics. accepted for publication in *Ocean Dynamics*.
- Spall, M. and J.F. Price 1998. Mesoscale variability in denmark strait: the pv outflow hypothesis *J. Phys. Ocean.* 28:1598-1623.
- Stashchuk, N. and K. Hutter 2001. Modelling of water exchange through the Strait of the Dardanelles. *Continental Shelf Research* 21: 1361-1382.
- Stern, M., Whitehead, J. and B. Hua 1982. The intrusion of a density current along the coast of a rotating fluid. *J. Fluid Mech.* 123: 237-265.
- Tutsak, E. 2013. Analyses of marine and atmospheric observations along the Turkish Coast, Institute of Marine Sciences, Middle East Technical University, Erdemli, Mersin, Turkey, Masters thesis 125 pp.
- Ünlüata, Ü., Oğuz, T., Latif, M.A. and E. Özsoy 1990. On the physical oceanography of the Turkish Straits. In: L.J. Pratt (Ed) *The Physical Oceanography of Sea Straits* NATO/ASI Series, Kluwer, Dordrecht, 25-60 pp.